Flammability and Thermal Degradation Behaviors of Phosphorus-Containing Copolyester/$BaSO_4$ Nanocomposites

Ming-Hai Qu, Yu-Zhong Wang, Ya Liu, Xin-Guo Ge, De-Yi Wang, Chuan Wang

Center for Degradable and Flame-Retardant Polymeric Materials, College of Chemistry, Sichuan University, Chengdu 610064, China

Received 10 July 2005; accepted 21 February 2006
DOI 10.1002/app.24304
Published online in Wiley InterScience (www.interscience.wiley.com).

ABSTRACT: A novel phosphorus-containing copolyester (PET-*co*-DDP)/barium sulfate ($BaSO_4$) nanocomposite was synthesized by *in situ* polymerization. The oxygen index values of the resulting nanocomposites decreased with increasing the content of $BaSO_4$ nanoparticles, but their antidripping behaviors were improved obviously through the UL-94 test. The flammability tests based on the cone calorimetry showed that the introduction of nano-$BaSO_4$ to the copolyester decreased remarkably the heat release rate and effective heat of combustion. The thermal oxidative decomposition behaviors of PET-*co*-DDP/$BaSO_4$ nanocomposites were studied by a conventional dynamic thermogravimetric analysis in a flowing air atmosphere with a heating rate of 20°C/min. The activation energies determined from Kissinger method, Flynn-Wall-Ozawa method, and Friedman method had a same variation trend. © 2006 Wiley Periodicals, Inc. J Appl Polym Sci 102: 564–570, 2006

Key words: flame retardance; thermogravimetric analysis (TGA); antidripping; nanocomposites

INTRODUCTION

Phosphorus-containing copolyesters are increasingly gaining popularity because of to their excellent flame retardancy, which is attributed mainly to melt dripping so as to enhance the loss of heat and material from the surface of the burning copolyesters. In most cases, therefore, the melt dripping phenomenon is very serious during the combustion of the polyesters,[1–8] meaning that their flame retardancy conflicts with their antidripping or nondripping behaviors. In fact, the melt dripping of flame-retardant products is a disadvantage in many cases such as flame-retardant clothing, causing the scald of the bodies or second fire. There are some literatures that are concerned about the fire-proofing and nondripping properties of polyalkylene terephthalate and polypropylene.[9–11] However, there are seldom literatures reporting nondripping or antidropping flame retardant additives aimed at polyethylene terephthalate (PET). It is necessary to design and synthesize highly efficient flame retardants for PET, which combine nondripping and flame retardancy.

In recent years, nanostructured inorganic–organic composites have attracted increasing interests of researchers. They exhibit improved performances compared with those of conventional composites because their unique phase morphology maximizes interfacial contact between the inorganic and organic phases and enhanced interfacial properties. Inorganic–organic nanocomposites greatly improve the thermal and mechanical barrier and even the flame-retardant properties of the polymers.[12]

In this work, we synthesized a novel nanocomposite by *in situ* polymerization of terephthalic acid (TPA), ethylene glycol (EG), 9,10-dihydro-10 [2,3-di (hydroxy carbonyl) propyl] 10-phosphaphenanthrene-10-oxide (DDP), and $BaSO_4$ nanoparticles prepared by reacting H_2SO_4 with $Ba(OH)_2$ in EG. The flammability and melt dripping behaviors of the resulting PET-*co*-DDP copolyester/$BaSO_4$ nanocomposites were investigated, and their thermal degradation behaviors were also studied and compared with PET and PET-*co*-DDP. Their crystallization, rheological, and mechanical properties will be reported in another article.

EXPERIMENTAL

Materials

Terephthalic acid (TPA), ethylene glycol (EG), and Sb_2O_3 were supplied by Jinan Zhenghao Advanced

Correspondence to: Y.-Z. Wang (yzwang@mail.sc.cninfo.net).
Contract grant sponsor: National Science Foundation of China; contract grant number: 50173016.
Contract grant sponsor: National Science Fund for Distinguished Young Scholars; contract grant sponsor: 50525309.
Contract grant sponsor: 863 Program of China; contract grant number: 2003AA302550.

TABLE I
Basic Physical Properties of Copolyesters

Sample	DDP% (w/w)	$BaSO_4$% (w/w)	[η] (dL/g)	DEG (%)	—COOH (mol/t)
PET	0	0	0.658	4.8	3.1
PET-1	10	0	0.654	4.0	33.4
PET-2	10	3	0.646	3.8	29.2
PET-3	10	5	0.650	4.1	30.1

Fiber Co. (Jinan, China). 9,10-Dihydro-10 [2,3-di (hydroxy carbonyl) propyl] 10-phosphaphenanthrene-10-oxide (DDP) was provided by Weili Flame Retardant Chemicals Industry Co. (Chengdu, China). $Ba(OH)_2{\cdot}8H_2O$ and H_2SO_4 (98 wt %) were commercially available and used as received.

Preparation of nano-$BaSO_4$ suspensions

$Ba(OH)_2{\cdot}8H_2O$ was dissolved in EG at 80°C with stirring, then H_2SO_4 (98 wt %) diluted with EG was added while stirring vigorously. The suspension was continued to stir for 30 min, then transferred into a flask equipped with a distillation column, and heated slowly to 190°C to remove water. Thus nano-$BaSO_4$ suspension was obtained.

Preparation of PET-*co*-DDP/$BaSO_4$ nanocomposites

TPA, EG, DDP, and Sb_2O_3 were introduced in a homemade 10 L reactor equipped with a nitrogen inlet, a condenser, and a mechanical stirrer. The reactor was heated in nitrogen atmosphere to 235°C under a pressure of 0.3 MPa and maintained for 2.5 h. Then the temperature was raised to 260–270°C, and the pressure was reduced to air pressure. Under a steady stream of N_2 gas, the nano-$BaSO_4$ suspension was added slowly to the mixture while maintaining the temperature above 230°C. In this condition, the excess EG was drained out from the condenser. Afterwards, the mixture was heated slowly to 270°C, and during this period, the excess EG of the mixture was continued to be distilled. Subsequently, the temperature of the mixture raised, meanwhile, the pressure decreased. Finally, the mixture was reacted at 280–285°C under a pressure of less than 50 Pa for 2 h, and then the polymerization was completed. The resulting polymer melts were extruded at the N_2 pressure and cooled with water.

PET-*co*-DDP was prepared from TPA, EG, and DDP by the conventional polymerization method.[8] The basic parameters of these copolyesters are given in Table I.

Characterization

The intrinsic viscosity (IV) of these copolyesters was determined with a Ubbelohde viscometer in phenol and 1,1,2,2-tetrachloroethane (1 : 1 w/w) solution. The carboxyl-terminal group was measured by titrimetry. The content of DEG was measured on an HP6890 gas chromatographic instrument. The sample was dissolved in phenol and 1,1,2,2-tetrachloroethane (1 : 1 w/w), and 1 μL of solution was injected. On the basis of the detention period, we can gain the peak area of DEG of the sample. Then the content of DEG was calculated by the following formula:

$$\text{DEG } \% = A_1/A_2 \times f \times 5 \times 100\%$$

where A_1 and A_2 are the peak area of DEG of the sample and the peak area of DEG of the standard sample, respectively, and f is the correction coefficient (1.421).

TEM images of the nanocomposite specimens without staining were taken at room temperature on a Jeol 100CX II transmission electron microscope operated at 120 kV. The TEM specimens were cut from epoxy block with the embedded nanocomposites at low temperature, using an ultramicrotome (Ultracut-1, U.K.) with a diamond knife.

SEM measured on a Hitachi 450 was used to investigate the surface of residues of samples and operated at 75 kV. SEM graphs of the residual char samples were recorded after gold surface coating.

The limiting oxygen index (LOI) test was performed according to the testing procedure of ISO4589–1984. To study the melt dripping behavior, a UL-94 flame test procedure was used. All flame tests were done in a CZF-2 General UL-94 flame test station. All test bars underwent two trials, each trial consisting of ignition for 10 s, followed by flame removal, and the time for self-extinguishing and dripping characteristics were recorded.[13]

The flammability was measured with a fire testing technology limited cone calorimeter at an incident heat flux of 35 kW/m^2 in accordance with ASTM E 1356. The standard uncertainty of the measured heat release rate (HRR) was ±10%. The experimental data were analyzed with Excel and Origin. All tests were run in the horizontal orientation. For each group of modified polyesters, at least 10 specimens were tested, all having the same dimensions of 12.5 × 12.5 × 0.3 cm^3.

TGA was performed with a DuPont 951 instrument coupled to a 1050 thermal analyzer. The measurements (10 ± 3 mg) were stacked in an open platinum sample pan and the experiment was conducted in air atmosphere at a flow rate of 80 mL/min with various heating rates (i.e., 10, 20, 30, 40°C/min). Continuous records of sample temperature, sample weight, and its first derivative were taken.

Kinetic methods

Kinetic information can be extracted from dynamic experiments by means of various methods. All kinetic studies assume that the isothermal rate of conversion, $d\alpha/dt$, is a linear function of a temperature-dependent rate constant, k, and a temperature-independent function of the conversion, α, that is:

$$\frac{d\alpha}{dt} = kf(\alpha) \tag{1}$$

where $f(\alpha)$ depends on the particular decomposition mechanism. In the case of polymer degradation, it is usually assumed that the rate of conversion is proportional to the concentration of material that has been reacted. Therefore,

$$f(\alpha) = (1-\alpha)^n \tag{2}$$

where n is the order of the reaction.

According to Arrhenius,

$$k = Ae^{-E/RT} \tag{3}$$

where A, the pre-exponential factor, is assumed to be independent of temperature, E is the activation energy, T the absolute temperature, and R the gas constant.

Combination of eqs. (1), (2), and (3) gives

$$\frac{d\alpha}{dt} = A(1-\alpha)^n e^{E/RT} \tag{4}$$

If the sample temperature is changed at a controlled and constant heating rate, $\beta = dT/dt$, the variation in the conversion can be analyzed as a function of temperature, this temperature being dependent on the time of heating. Therefore, the reaction rate may be written as follows:

$$\frac{d\alpha}{dt} = \frac{d\alpha}{dT}\frac{dT}{dt} = \beta\frac{d\alpha}{dT} \tag{5}$$

A combination of eqs. (4) and (5) leads to

$$\frac{d\alpha}{dT} = \frac{A}{\beta}e^{E/RT}(1-\alpha)^n \tag{6}$$

The Kissinger method,[14] Flynn-Wall-Ozawa method,[15] and Friedman method[16] have been used in the literature to determine the activation energy.

RESULTS AND DISCUSSION

Physical characteristics and morphology of nanocomposites

As can be seen from Table I, the IV and the DEG content of the nanocomposites are almost the same as those of PET and PET-*co*-DDP, proving that addition of nano-$BaSO_4$ has no significant effect on the polymerization process. The higher content of carboxyl terminal group of the PET-*co*-DDP and nanocomposites is due to the acidic flame retardant DDP. It is well known that the dispersion of the filled particles in the polymers significantly affects the properties of the composites, and that inorganic nanoparticles are hard to be dispersed in polymer matrices because of particle agglomeration and immiscibility between the inorganic particles and the polymer matrix. However, in this study, a good dispersion of $BaSO_4$ in the polymer matrix can be obtained, and the nanoscale dispersion morphology of the resulting composites was observed by TEM as shown in Figure 1. The nanoparticles were well dispersed in the polymer matrix when the filler concentration is lower, having an average particle size of about 80 nm. However, the nanoparticles formed the clusters or agglomerated structures in the matrix with high filler concentrations, and had bigger particle sizes, even over 200 nm. It is reasonable to think that in the case of higher concentration of $BaSO_4$ nanoparticles, the distance between the particles is smaller, so these particles are easy to aggregate.

Flammability and thermal analysis

The percentage of oxygen in the O_2 and N_2 mixture, just sufficient to sustain the flame, is taken as the LOI. The LOI value could be used to estimate the flame retardancy of materials. The LOI values of these samples are shown in Table II. As shown in Table II, the nanocomposites had lower LOI values compared with the PET-*co*-DDP under the same content of DDP, and the LOI values of nanocomposites, though high enough to self-extinguish in air, decrease with the increase of $BaSO_4$ nanoparticle content. Nevertheless, UL-94 testing results displayed a reversed trend. That is, with the increase of nano-$BaSO_4$ content, the nanocomposites have an improved UL-94 testing behavior, reaching a UL-94 V-0 rating and 0 s of extinguishing time when containing 5 wt % of $BaSO_4$ and 10 wt % of DDP. Furthermore, the melt dripping of the samples was obviously improved.

Figure 2 shows the TG curves of PET, PET-*co*-DDP, and two kinds of phosphorus-containing nanocomposites at a heating rate of 20°C/min in air. Table III gives the characteristic decomposition temperatures of various samples from Figure 2. We can see that the initial decomposition temperature (T_{di}), at which the weight loss of samples reaches 5 wt %, and the max-

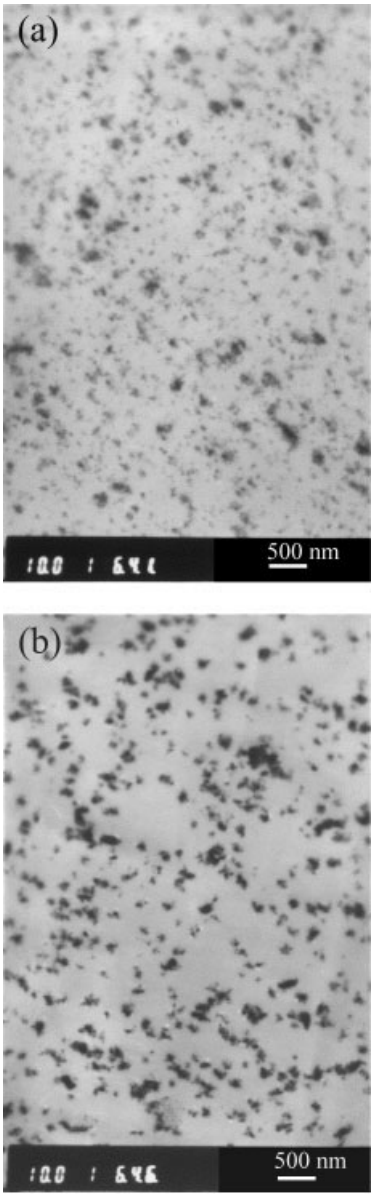

Figure 1 TEM micrograph of PET-*co*-DDP/$BaSO_4$ nanocomposites: (a) PET-2 and (b) PET-3.

imum-decomposing-rate temperature (T_{max}), at which the decomposing rate reaches a maximum, have a little change between the samples. Therefore, the addition of the nanoparticles did not increase the thermal oxidative stability. However, the residues of thermal oxidative degradation of PET, PET-1, and PET-2 at the heating rate of 20°C/min are quite different (see Table IV). Above 450°C, PET-2 has higher residue than PET and PET-1, even if the $BaSO_4$ content in the copolyester was deducted from the residue. This phenomenon is quite likely to be associated with the charring effect in air at high temperatures. When the samples are heated and ignited, the nano-$BaSO_4$ particles concentrate to the surface of the material as a result of their high surface energy. The nanoparticles are not ignited during fire and can be fixed in the material by the liquid phosphorus-containing char in the flame. Just as shown in Figure 6(a), there were some small holes on the residual surface, while these cannot be found in Figure 6(b) and even under high multiple of Figure 7(a). Meanwhile, Figure 7(b) showed that the surface of fracture was very compact. The $BaSO_4$-containing char layers perform better at holding back the transport of heat and mass than the charring layers only containing phosphorus. At the

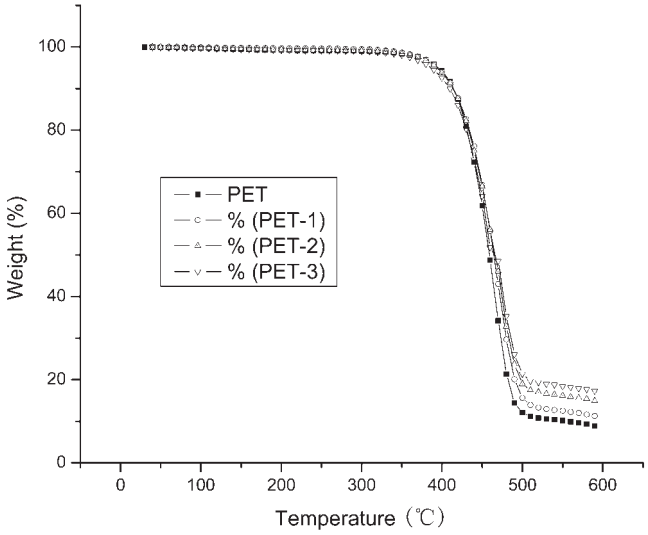

Figure 2 TG curves of various polyesters at a heating rate of 20°C/min in air condition.

TABLE II
Flame Test Results of the Nanocomposites

Samples	LOI (%)	UL-94 flame test results			
		Self-extinguishing time (s) for first ignition[a]	Self-extinguishing time (s) for second ignition[a]	Observed dripping[b]	UL-94 rating
PET	21	>150	None	>100	No result
PET-1	32	21	5.6	>100	V-2
PET-2	30	7.1	1	46	V-2
PET-3	28.5	0	0	16	V-0

[a] The total time of five specimens to self-extinguishing after ignition.
[b] Total dripping time of five specimens from heating to self-extinguishing.

TABLE III
T_{di} and T_{max} of Copolyesters Determined From TG Curves (Heating Rate: 20°C/min)

Sample	T_{di} (°C)	T_{max} (°C)
PET	395	472
PET-1	396	464
PET-2	387	467
PET-3	393	472

T_{di}, the initial decomposing temperature; T_{max}, the maximum-decomposing-rate temperature.

same time, this kind of $BaSO_4$-containing char layers have superior high temperature stability because of the existence of nanoparticles, resulting in an improvement of the thermal insulation of the nanocomposites.

On the other hand, the cone calorimeter gave the further flammability information of various samples. HRR, effective heat of combustion (EHC), and mass loss rate (MLR) curves of PET, PET-1 and PET-3 are shown in Figures 3, 4, and 5, respectively. Combustion properties of samples are shown in Table V. The results show that the nanocomposite samples slightly increase the time to ignition (TTI) and significantly reduce the peak heat release rate (pk-HRR) and peak effective heat of combustion (pk-EHC) in comparison to PET and PET-1. Compared to PET, the pk-HRR of PET-1 decreased from 1013 to 744 kw/m^2, while the pk-HRR of PET-3 decreased to 424 kw/m^2, i.e., 42.9% and 58.1% lower than that of PET-1 and PET, respectively. From Figure 5, we can see that after the burning finished, the residues of PET, PET-1, and PET-3 were 9.2%, 14.7%, and 43.7%, respectively, that is, the residue of PET-3 was increased sharply.

The above phenomena may be explained as follows. When the samples are ignited, the P—O bond starts to decompose and the protective phosphorus–carbon layer begins to form. The nano-$BaSO_4$ particles begin to migrate to the surface of the material because of their high surface energy. Because of the existence of the nanoparticles, the charring layer is becoming substantial and continuous, which can be seen from Figure 6 and Figure 7. The charring layer could hold back the pyrolyzed flammable gases to reach the fire, and isolate the heat away from the unburned matrix. And also the charring layer might decompose further during the process of burning.

TABLE IV
Residues of Thermal Oxidative Degradation of PET, PET-1, PET-2 (Heating Rate: 20°C/min)

Temperature (°C)	Residue of copolyesters (wt %)		
	PET	PET-1	PET-2
490	14.42	20.13	23.78
510	11.20	13.94	17.48
530	10.58	13.00	16.62
550	10.16	12.53	16.15
570	9.645	11.99	15.59
590	8.914	11.27	14.89

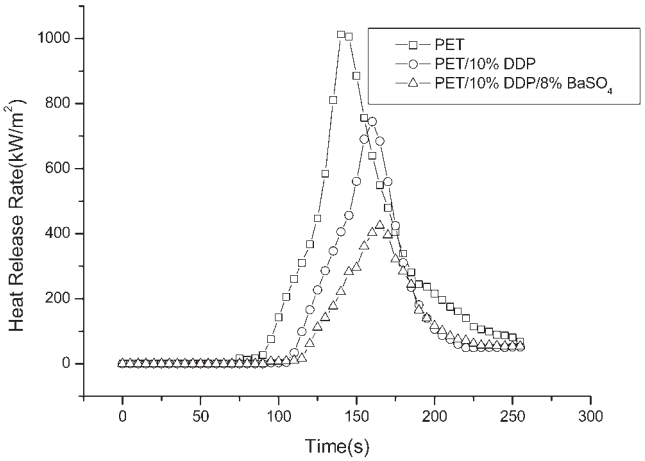

Figure 3 The HRR curves of samples.

Thermogravimetric analysis (TGA) is one of the techniques used widely for rapid evaluation of the thermal stability of different materials, and can also indicate the decomposition of polymers at various temperatures. Thermal oxidative degradation is a complex process, and there are wide variations in the apparent activation energies calculated according to different mathematical approaches taken in the analysis. Kissinger, Ozawa, and Friedman calculations are applicable to all points on the TG curves. First, we used Kissinger method to calculate the activation energy for different polyesters. The results are listed in Table VI. According to the calculated results, PET-1

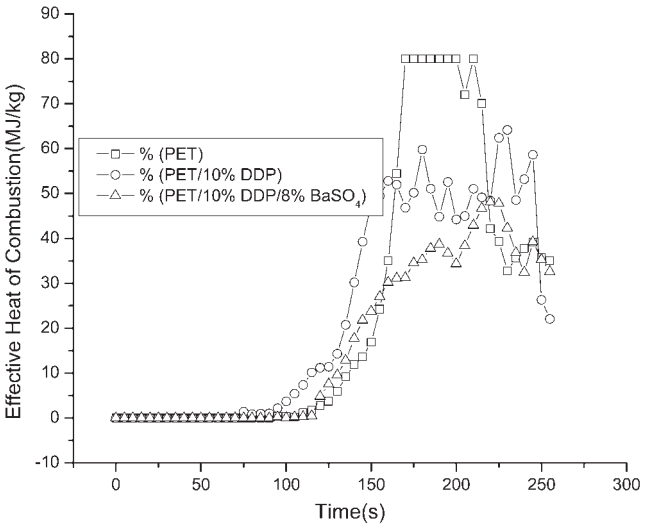

Figure 4 The EHC curves of samples.

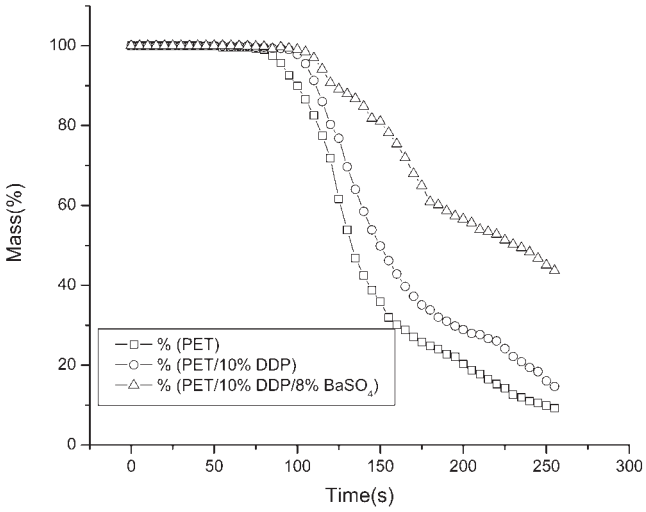

Figure 5 Weight loss curves of samples during combustion.

has the highest activation energy; the addition of nano-$BaSO_4$ leads to the decrease of activation energy of polyesters, which agrees with the decrease of LOI values.

Second, we also used Friedman method by plotting ln ($d\alpha/dt$) against $1/T$ for a constant α value and calculated the activation energy. Analyzing the data, we find that PET-1 has higher activation energies, which are in accordance with the results obtained from Kissinger method.

Ozawa method was used to obtain the activation energies for different conversion values by fitting the plots of log β versus $1/T$. The fitting straight lines are nearly parallel, thus indicating the applicability of Ozawa method to the systems in the conversion range investigated.

All the three methods lead to the conclusion that the incorporation of phosphorus linkage into the pendant group would increase the activation energy and LOI value; however, the introduction of nano-$BaSO_4$ into the copolyesters causes a considerable decrease in the activation energy of thermal oxidative degradation, which was contrary to PET-*co*-DDP/MMT nanocomposites.[17] The lower LOI values may be associated with the decreased activation energy. However, we can see from the T_{max} data that the lower activation energy does not decrease the thermal stability of the nanocomposites.

As shown above, there is a strong correlation between the activation energy and the LOI values: the greater the activation energy, the higher the LOI value. However, the char yields of the nanocomposites

TABLE V
Combustion Properties of Samples

Sample	TTI (s)	pk-HRR (kW/m^2)	av-HRR (kW/m^2)	pk-EHC (MJ/kg)	av-EHC (MJ/kg)
PET	75	1013	322	80	36
PET-1	93	744	227	64	34
PET-3	95	424	152	48	26

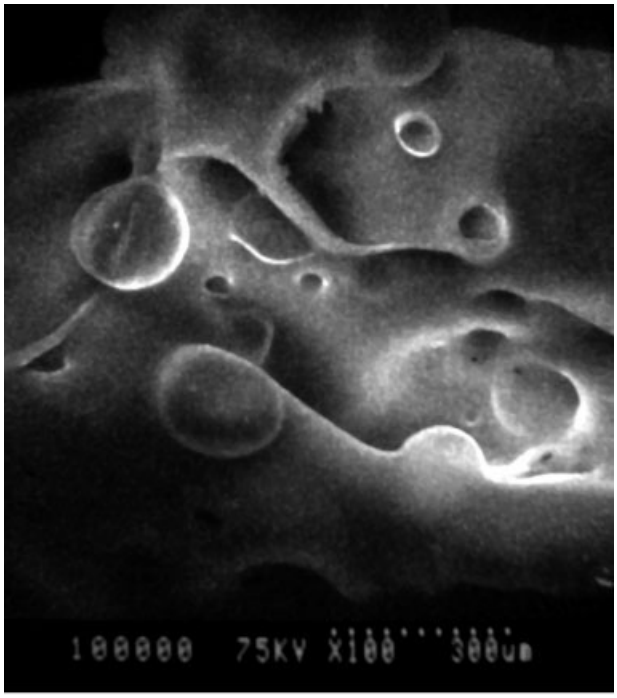

(a)

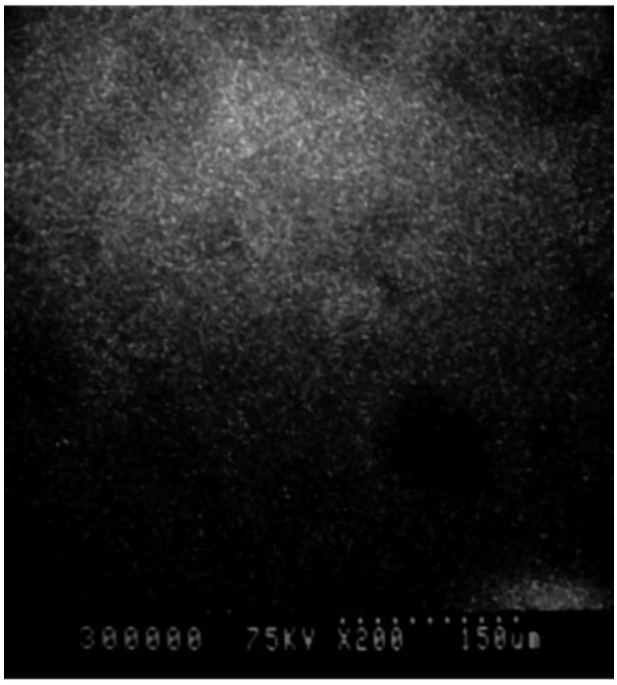

(b)

Figure 6 SEM image of char layer of samples: (a) PET-1 and (b) PET-2.

were higher than those of PET-*co*-DDP. All those facts suggest that there is a synergistic effect between the flame-retardant elements and the nanoparticles. The introduction of the nano-$BaSO_4$ did not decrease the thermal oxidative stability, but improved the anti-dropping behavior of copolyesters.

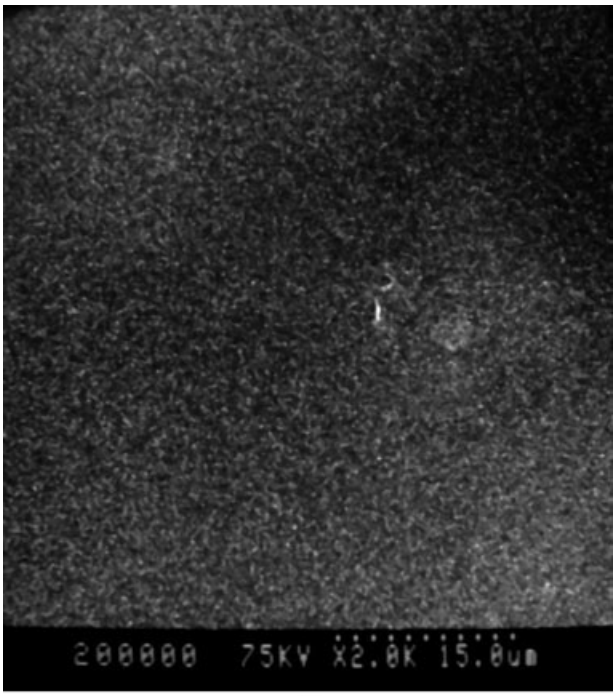

(a)

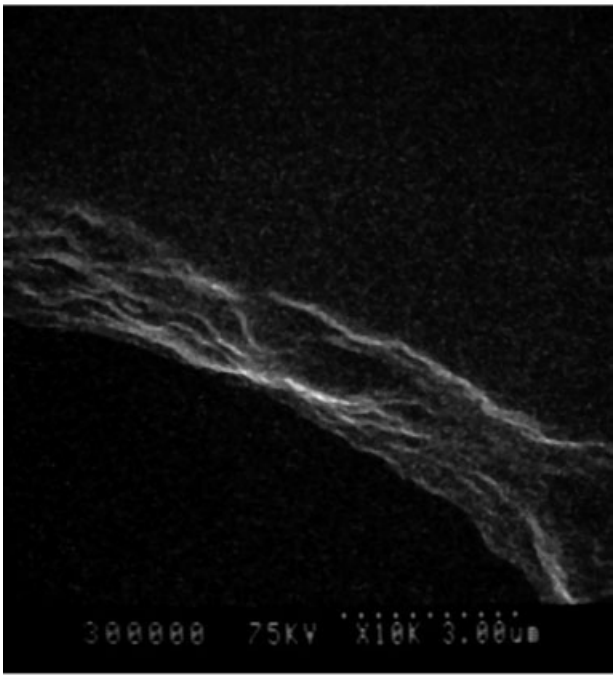

(b)

Figure 7 SEM image of char layer of PET-3: (a) high multiple and (b) image of the surface of fracture.

TABLE VI
Calculated Activation Energies by Kissinger's Method

Samples	Activation energies (kJ/mol)	Correlation coefficient (r)
PET	134	0.99752
PET-1	144	0.97906
PET-2	127	0.9901
PET-3	133	0.99932

CONCLUSIONS

The phosphorus-containing copolyester (PET-*co*-DDP)/barium sulfate ($BaSO_4$) nanocomposite can be synthesized by *in situ* polymerization of TPA, EG, DDP, and $BaSO_4$ nanoparticles, which were prepared by reacting H_2SO_4 with $Ba(OH)_2$ in EG. A nanoscale dispersion of the $BaSO_4$ particles in the copolyester matrix can be reached. The dispersion of the $BaSO_4$ particles in the PET matrix has an important effect on the flammability of the nanocomposites, but the thermal oxidative stability of nanocomposites has no obvious change when compared with those of PET-*co*-DDP and PET. The methods of Kissinger, Friedman, and Ozawa show excellent applicability to the kinetic description of thermal oxidative degradation of the nanocomposites. It has been proved that the nanocomposites have lower LOI values and activation energy than PET-*co*-DDP. On the other hand, the nanocomposites have higher residues, much lower peak heat release rate and pk-EHC than PET-*co*-DDP and PET. All those indicate that the introduction of nano-$BaSO_4$ can enhance the charring ability of the copolyesters and improve antidropping behavior of the materials without the decrease of thermal stability.

References

1. Wang, C. S.; Shieh, J. Y.; Sun, Y. M. J Appl Polym Sci 1998, 70, 1959.
2. Wang, C. S.; Lin, C. H. Polymer 1999, 40, 747.
3. Liu, Y. L. Polymer 2001, 42, 3445.
4. Shieh, J. Y.; Wang, C. S. Polymer 2001, 42, 7617.
5. Chen, X. T.; Tang, X. D.; Wang, Y. Z. Chem J Chinese Univ 2002, 23, 508.
6. Wang, Y. Z. Flame Retardation Design of PET Fibers; Sichuan Science and Technology Press: Chengdu, 1994.
7. Wu, B.; Wang, Y. Z.; Wang, X. L.; Yang, K. K.; Jin, Y. D.; Zhao, H. Polym Degrad Stab 2002, 76, 401.
8. Chang, N. J.; Chang, F. C. J Appl Polym Sci 1999, 72, 109.
9. Ott, K. H.; Fuhr, K.; Mueller, F. U.S. Pat. 5,191,000 (1993).
10. Gray, A. R. U.S. Pat. 3,936,420 (1976).
11. Yutaka, E.; Tadayuki, I. Jpn.Pat. 11,209,601 (1999).
12. Gilman, J. W.; Kashiwagi, T.; Lomakin, S.; Lichtenhan, J. D.; Jones, P.; Giannelis, E. P.; Manias, E. Proceedings of the International Wire and Cable Symposium 1997, 46, 761.
13. Vandersall, H. L. J Fire Flamm 1971, 2, 97.
14. Kissinger, H. E. Anal Chem 1957, 29, 1702.
15. Ozawa, T. Bull Chem Soc Jpn 1965, 38, 1881.
16. Fridman, H. L. J Polym Sci Part C: Polym Symp 1964, 6, 183.
17. Wang, D. E.; Wang, Y. Z.; Wang, J. S.; Chen, D. Q.; Zhou, Q.; Yang, B.; Li, W. Y. Polym Degrad Stab 2005, 87, 171.